

# Microdosimetric Measurements in gamma and neutron fields with a Tissue Equivalent Proportional Counter (TEPC) based on a Gas Electron Multiplier (GEM)

L. De Nardo<sup>1,2,\*</sup>, F. Dal Corso<sup>2</sup>, M. Pegoraro<sup>2</sup>

<sup>1</sup>University of Padova, Physics and Astronomy Department, via Marzolo 8, I-35131 Padova, Italy

<sup>2</sup>PD-INFN, via Marzolo 8, I-35131 Padova, Italy

\* Corresponding author:

Telephone: +39-049-8277210

Fax: +39-049-8277102

email: laura.denardo@unipd.it

Running title: Microdosimetry with a GEM-TEPC

*This is a pre-copyedited, author-produced PDF of an article accepted for publication in Radiation Protection Dosimetry following peer review. The version of record [L. De Nardo, F. Dal Corso, M. Pegoraro; Microdosimetric Measurements in Gamma and neutron Fields with a Tissue Equivalent Proportional Counter Based on a Gas Electron Multiplier. Radiat Prot Dosimetry 2017; 175 (2): 260-266. doi: 10.1093/rpd/ncw294] is available online at:*

<https://academic.oup.com/rpd/article-abstract/175/2/260/2558993/Microdosimetric-Measurements-in-Gamma-and-neutron>

# Microdosimetric Measurements in gamma and neutron fields with a Tissue Equivalent Proportional Counter (TEPC) based on a Gas Electron Multiplier (GEM)

L. De Nardo, F. Dal Corso, M. Pegoraro

## ABSTRACT

A multi-element Tissue-Equivalent Proportional Counter (TEPC), based on a single GEM foil of standard geometry, has been constructed with 16 cylindrical sensitive volumes. In this paper, the design of this novel counter is described and first microdosimetric measurements are presented. To study the response of the GEM-TEPC to both low and high LET radiation fields, the microdosimetric spectra due to a  $^{137}\text{Cs}$  gamma-ray source and to fast neutrons from  $^7\text{Li}(d,n)^8\text{Be}$  reaction have been measured using pure propane gas at low pressure, in order to simulate a tissue site of about  $1\ \mu\text{m}$  equivalent size. The comparison with spectra measured with a spherical TEPC and with a mini-TEPC demonstrates promising properties for application of the GEM-TEPC for microdosimetric applications.

**Keywords:** Microdosimetry, TEPC, GEM, Proportional counter

---

## INTRODUCTION

The Tissue-Equivalent Proportional Counter (TEPC) is the reference instrument to measure the statistical distribution of energy-deposition events at a microscopic level<sup>(1)</sup>. This allow to assess the effects of ionising radiation on biological targets by weighting the measured spectra through appropriate weighting functions<sup>(2)</sup> or by extracting relevant microdosimetric parameters such as the dose-mean lineal energy,  $\overline{y_D}$ , or the saturation-corrected dose-mean lineal energy,  $y^*$ <sup>(1)</sup>.

A traditional TEPC is a proportional counter with a central anode wire operated with a tissue-equivalent (TE) gas mixture. Commercial TEPC are spherical counter with a diameter of a few centimeters and their large size does not allow to attain a good spatial resolution. Besides, in high dose-rate radiation fields such as those employed in radiotherapy, pile-up of the electronic signals causes spectrum distortion and large dead time<sup>(3)</sup>. To reduce these effects, the physical dimension of a TEPC must be minimized. In the last two decades, several groups have developed various types of miniaturized TEPCs (mini-TEPCs)<sup>(4-7)</sup>, by reducing the dimensions of all components of a conventional TEPC and employing a cylindrical geometry rather than the usual spherical one. The spherical geometry is usually preferred because it guarantees an isotropic response and because of the lowest relative variance of the chord length distribution<sup>(8)</sup>. Even if the mean chord length of a right cylinder with height equal to diameter  $d$  is the same as that of a sphere of diameter  $d$ , namely  $\bar{l}=2d/3$ , their chord length distributions differs slightly, but this difference does not significantly influence the single event spectrum<sup>(9-10)</sup>.

Yet mini-TEPC are fairly complex and difficult to use<sup>(7)</sup>. For these reasons, efforts have also been made for developing simple, easy-of-use, transportable and cheap instruments to measure microdosimetric distributions in hadron beams, such as silicon microdosimeters<sup>(11-12)</sup> and chemical vapour deposition diamond (CVD) microdosimeters<sup>(13)</sup>.

Some attempts have also been made to develop TEPCs based on Gas Electron Multiplier (GEM)<sup>(14)</sup> or Thick Gas Electron Multiplier (THGEM), both for radiotherapy and radioprotection application<sup>(15-17)</sup>. The application of a GEM for the design of a microdosimetric detector has the advantage to simplify the construction both of a miniature counter with a small sensitive volume, to reduce pile-up effects<sup>(15)</sup> and that of a multi-element counter, to increase the sensitivity of the TEPC to measure at low dose rates<sup>(16)</sup>.

In this work, a multi-element TEPC, based on a single GEM foil of standard geometry as multiplying element, developed for hadrontherapy application, is described and first microdosimetric measurements performed with this instrument are presented. Similarly to the design of Dubeau and Waker<sup>(16)</sup>, the collection volumes are without side-walls and are defined by the size of the collecting anode pads. This design allow to simplify the construction of the counter and, at the same time, to reduce the deformation of microdosimetric spectra due to the so-called "wall-effects" generated by delta rays<sup>(18)</sup>, important mainly for high energy charged particles such as those employed in hadrontherapy<sup>(19)</sup>. Differently by the design of Dubeau and Waker<sup>(16)</sup>, in this detector yet the charge collected on different pads can be acquired independently, opening the experimental way to a two dimensional microdosimetric mapping of a radiation field.

## METHODS AND MATERIALS

### Experimental setup

The GEM-TEPC is a multi-element proportional counter, which main elements are a cathode, made of A-150 plastic 1 mm-thick, a GEM foil and a readout printed circuit board (PCB). The drift region

(space between cathode and GEM) and the induction region (space between GEM and PCB) have a height of 2 mm and 0.5 mm, respectively. Figure 1 provides a schematic view of the counter. The GEM structure used in this work is the so called standard GEM, that is a Kapton foil of 50  $\mu\text{m}$  thickness, with a 5  $\mu\text{m}$ -thick copper coating on each side, perforated on a triangular pattern with a high density of holes with a double conical shape. The diameter in the copper surfaces is 70  $\mu\text{m}$ , the diameter in the Kapton is 50  $\mu\text{m}$ . The holes have a distance between the centers of 140  $\mu\text{m}$ . The sensitive area of the GEM is  $5 \times 5 \text{ cm}^2$ . The GEM foil is glued between two fiberglass frames, each one of 0.5 mm thickness. The PCB is composed of a large electrode, necessary to properly define the electric field in the induction region, and 16 circular pads of 2 mm diameter, disposed in a  $4 \times 4$  matrix (pitch of 4 mm), isolated from the large electrode by guard rings of 0.2 mm thickness. Each pad has its own electrical connection, allowing to collect independently the charge released inside 16 cylindrical sensitive volumes (SVs) of 2 mm height and diameter. The GEM and the PCB were produced at the CERN printed circuits workshop. The detector is inserted in a vacuum tight chamber, holding the hermetic feedthroughs for the high voltages and the signal lines and for gas inlet and outlet. On one side of the chamber, in correspondence of the position of the detector's SVs, there is a flange with a Kapton window of 25  $\mu\text{m}$  thickness which provide the entrance channel for the accelerated beam. As the gas purity is an important factor which can greatly influence the stability of the gas gain and the reproducibility of the measurements, the chamber was operated with a continuous flow supply system of pure propane gas ( $\text{C}_3\text{H}_8$ ). The advantage provided by the use of  $\text{C}_3\text{H}_8$  with respect to that of gas mixtures commonly employed in microdosimetry, that is propane- and methane-based TE gas mixtures, has been discussed in a previous paper<sup>(20)</sup>. Measurements have been performed at 21 and 28 kPa of  $\text{C}_3\text{H}_8$  gas, corresponding to a mass thickness of the SV of  $0.75 \cdot 10^{-3} \text{ kg} \cdot \text{m}^{-2}$  and  $1 \cdot 10^{-3} \text{ kg} \cdot \text{m}^{-2}$  at  $20^\circ\text{C}$ . As the equivalence of microdosimetric spectra measured in TE- $\text{C}_3\text{H}_8$  and pure  $\text{C}_3\text{H}_8$  has been proven when the gas density of pure  $\text{C}_3\text{H}_8$  is reduced by a factor 0.75 as compared to TE- $\text{C}_3\text{H}_8$  in order to get the same equivalent site size<sup>(21)</sup>, microdosimetric spectra acquired in this work should correspond to microdosimetric spectra measured with TE- $\text{C}_3\text{H}_8$  at 1  $\mu\text{m}$  and 1.3  $\mu\text{m}$  equivalent site size.

The readout board was grounded and high voltages, with negative polarity, were supplied to the drift electrode and the two sides of the GEM through independent outputs of a CAEN DT5521 Desktop Power Supply through 2 M $\Omega$  protection resistors connected in series with each electrode. In these measurements, the signals produced at four of the sixteen SVs were collected. The charge produced on 4 readout pads was fed into charge preamplifiers and pulses were then directly sent to a CAEN DT5724 Digitizer (4 Channel 14 bit 100 MS/s) equipped with DPP-PHA Firmware (Digital Pulse Processing for the Pulse Height Analysis) controlled by a PC. This provides a digital solution equivalent to shaping amplifier plus peak sensing ADC.

The detector has been tested with a  $^{137}\text{Cs}$  gamma-ray source and in a fast neutron beam at the CN Van de Graff accelerator of the Laboratori Nazionali di Legnaro of the Italian Institute of Nuclear Physics (LNL-INFN), by exploiting the reaction  $^7\text{Li}(d,n)^8\text{Be}$  ( $Q = 15.03 \text{ MeV}$ ), bombarding a lithium fluoride target of  $1 \cdot 10^{-2} \text{ kg} \cdot \text{m}^{-2}$  thickness with 5.5 MeV d beam. The beam current varied in the range  $180 \div 300 \text{ nA}$ .

### **Electric potential and electron collection efficiency calculations**

To assure a clear definition of the size of each SV of the counter it is necessary that electrons generated inside the drift gap move towards the GEM with a low transversal diffusion and that only the charge amplified in the region defined by the projection of the collecting pad on the GEM

plane is collected. To verify the fulfillment of these conditions, calculations of the electric field and simulations of the electron drift inside the counter have been performed. A numerical solution of the Laplace equation inside a model of the counter was obtained using the software FlexPDE 6 ([www.pdesolutions.com](http://www.pdesolutions.com)), a partial differential equations solver by the finite element method. A 3D geometric model of the GEM was created, by exploiting the inherent periodicity and symmetry of the structure<sup>(20)</sup>. Calculations performed for different values of  $\Delta V_{GEM}$  and of the drift and induction field,  $E_D$  and  $E_I$ , have shown that, although inside the GEM hole the electric field reaches very high values, the electric fields in the drift and induction regions becomes practically uniform at a distance of 0.1 mm from the top and bottom surfaces of the GEM, whatever the voltage difference between the two sides of the GEM,  $\Delta V_{GEM}$  (see Figure 2). Considering that the SV has a height of 2 mm, the approximation of uniform drift field can therefore be adopted to evaluate the collection efficiency of electrons generated inside the drift volume by means of a Monte Carlo code<sup>(22)</sup>. The term *electron collection efficiency* is here used to denote the probability that an electron released inside the nominal SV (cylinder of 2 mm diameter and height) drift close to the GEM foil, without diffusing outside the SV border. The collection efficiency of electrons inside the wall-less SV was calculated in C<sub>3</sub>H<sub>8</sub> gas at 21 and 28 kPa for different values of the drift field, considering an initial energy of the electrons of 2 eV. The collection efficiency,  $\epsilon$ , is quite uniform inside the SV, sharply decreasing to zero close to the SV border (see the efficiency map in Figure 3). The average efficiency  $\bar{\epsilon}$  has been found by integrating  $\epsilon$  inside the nominal SV border, by supposing electrons uniformly distributed inside the volume. It has been found that the average efficiency  $\bar{\epsilon}$  is about 91% and 94% respectively at 21 and 28 kPa, for typical values of the drift field. Calculations have also been performed for hypothetical SVs with lateral wall. In this situation the calculated efficiency was lower (about 86% and 88% at 21 and 28 kPa, respectively), supporting our choice to use SVs without lateral wall. These calculations do not take into account the electron transfer efficiency (transparency) through the GEM<sup>(23)</sup>, that is the probability that a drifting electron will enter into the GEM holes and will experience multiplication. However, on the base of calculations of the vertical component of the electric field on the drift facing electrode of the GEM, published in another paper<sup>(20)</sup>, it can be expected that, in our measurements conditions, the transparency will be close to 100%.

To assure that only the charge produced inside the SV and amplified by the GEM will be collected, a large electrode surrounds each collecting pad of the PCB, in order both to define a uniform electric field in the induction region and to collect the totality of the charge not coming from the SVs.

### Calibration of microdosimetric spectra

The measured pulse-height spectra were calibrated through the identification of a characteristic feature in the spectra themselves, the so-called proton-edge (p-edge), in the case of neutron measurements, and the so-called electron-edge (e-edge), in the case of gamma measurements. These edges correspond to the maximum amount of energy that an electron or a proton can deposit in the active volume of the detector,  $E_{max}$ , and the lineal energy at the edge,  $y_{edge}$ , can be calculated using the relation  $y_{edge} = E_{max} / \bar{l}$ , where  $\bar{l}$  is the mean chord length of the cavity.

When interacting with the TE plastic constituting the counter cathode, fast neutrons mainly collide with the hydrogen nuclei through elastic collisions, leading to the presence of a proton peak in the microdosimetric spectra, responsible for the majority of the absorbed dose, while the contribution of  $\alpha$  particles and heavy recoil ions (C, N, O) can be identified at higher lineal energies<sup>(24)</sup>. The p-edge can be distinctly identified in the measured spectra, allowing to calibrate the pulse-height spectra through the identification of this marker point and the assignment of a precise value of lineal energy to this marker.

In the case of gamma-ray sources, the maximum amount of energy is released by those electrons which cross the detector cavity along its longest chord,  $l_{max}$ , and stop exactly at the volume border (the so called "exact stoppers"). Despite the e-edge is less sharp than the p-edge, because of the larger energy and range straggling of electrons, the fast decrease in microdosimetric spectra of pure photon beams is also easily recognizable, allowing for spectra calibration.

The marker points in the measured spectra corresponding to the p-edge and e-edge positions have been identified following the recommendations given by Conte et al.<sup>(25)</sup>, by fitting the e- or p-edge region of each microdosimetric spectrum by a Fermi-like function. Afterwards, the intercept of the tangent through the inflection point of the Fermi function with the pulse height-axis,  $h_{TC}$ , was used as the marker point. The e-edge value has been found according to the indications of Moro et al.<sup>(26)</sup> and Chiriotti et al.<sup>(21)</sup>, obtaining the value of 15.5 and 13.9 keV/ $\mu$ m respectively for 1  $\mu$ m and 1.3  $\mu$ m equivalent site size. The p-edge value has been calculated by using the tables for stopping powers and ranges for protons given in ICRU Report 49<sup>(27)</sup>. The  $y_{p-edge}$  values were 147 and 144 keV/ $\mu$ m respectively for 1  $\mu$ m and 1.3  $\mu$ m equivalent site size.

## RESULTS

The microdosimetric spectrum measured by the GEM-TEPC with a  $^{137}\text{Cs}$  source at a simulated site of 1.3  $\mu$ m ( $P=28$  kPa), is plotted in Figure 4 and compared with a spectrum acquired by a large spherical TEPC<sup>(28)</sup>. The spectrum has been acquired with  $\Delta V_{GEM}$  equal to 440 V, obtaining a gas gain of approximately 3500<sup>(20)</sup> and a detection threshold of approximately 0.14 keV/ $\mu$ m. The rising and falling portion of the spectra measured by the two detectors are in good agreement, despite differences in the central part of the spectra. These differences can be due to the different geometry of the detectors and to the different irradiation conditions. In the case of the GEM-TEPC, the  $^{137}\text{Cs}$  source was in fact positioned over the cathode and therefore the radiation field was essentially monodirectional, while in measurements performed with the spherical TEPC two gamma source were employed, producing a more uniform radiation field.

In order to analyze the response of the counter at different gas gains, measurements in the neutron field due to the  $^7\text{Li}(d,n)^8\text{Be}$  reaction were performed for different values of  $\Delta V_{GEM}$ . In Figure 5 microdosimetric spectra at 1.0  $\mu$ m simulated size ( $P=21$  kPa), for  $\Delta V_{GEM}$  equal to 330, 350, 370 and 390 V, are plotted. Electric field strength in the drift and in the induction regions,  $E_D$  and  $E_I$ , were 45 kV/m and 300 kV/m respectively. With these configurations gas gain between 500 and 2000 was achieved<sup>(20)</sup>.

With increasing  $\Delta V_{GEM}$  the gain of the counter increases, allowing to measure a larger part of the spectrum in the lowest  $y$  region below 10 keV/ $\mu$ m, where events are generated by gamma rays. On the other hand, for  $\Delta V_{GEM}$  equal to 390 V, the spectrum is truncated at high  $y$  value, because the maximum height of the signals exceeds the dynamic range of the digitizer (2.25 Vpp).

Therefore it was not possible to increase further the gain to measure a larger part of the gamma portion of the spectra. The peak above 10 keV/μm up to approximately 150 keV/μm is due to proton recoils from elastic scattering caused by neutrons. The different shapes of this part of the spectra are due to different thresholds in the measured spectra. If the spectra are renormalized with a threshold at 3 keV/μm, all the spectra have the same shape (see Figure 6). The high-y events (above 150 keV/μm) result from heavy recoils of the TE material, mainly C and O ions. Apart for the spectrum acquired with  $\Delta V_{\text{GEM}}$  equal to 390 V, where the spectrum is truncated at high y value, this part of the spectra is independent of  $\Delta V_{\text{GEM}}$ , demonstrating that the detector correctly measures high LET radiations.

In these measurements, the signals produced at four of the sixteen SVs were collected at the same time. In Figure 7 spectra acquired for the different SVs are compared (1.0 μm simulated size,  $\Delta V_{\text{GEM}}$  equal to 370 V). Apart for small differences due to the different thresholds in the acquired channels, microdosimetric spectra measured for the different SVs were found to have the same shape. As the beam is uniform at their location, this proves that the different SVs behave at the same way, both for charge collection and amplification.

In Figure 8 microdosimetric spectra measured by the GEM-TEPC during two different runs of measurements are compared with spectra acquired by a large spherical TEPC<sup>(28)</sup> and by a cylindrical mini-TEPC<sup>(29)</sup> in the same neutron field. Measurements with the spherical TEPC have been performed in TE-C<sub>3</sub>H<sub>8</sub>, while those with the mini-TEPC have been performed in pure C<sub>3</sub>H<sub>8</sub>, as those with the GEM-TEPC. According to the equivalence criterion between microdosimetric spectra measured in TE-C<sub>3</sub>H<sub>8</sub> and pure C<sub>3</sub>H<sub>8</sub> established in the publication of Chiriotti et al.<sup>(21)</sup>, the equivalent site size of all the spectra is 1 μm. As spectra have different threshold and the low-y part of the spectra are different, probably because of a gamma field varying with time, due to the process of target activation, for the comparison the spectra have been scaled in order to obtain equal integral in the proton and heavy ion region ( $y > 10$  keV/μm). Spectra measured by the different counters show a very similar shape in the heavy ion peak. Spectra measured by the GEM-TEPC are also very similar to the spectrum acquired by the mini-TEPC, while some differences appear in the comparison with the spherical TEPC, which can be due to the different geometry of the detectors and the lower relative variance of the chord length distribution in the case of spherical counters.

Similar results have been obtained for measurements performed at 1.3 μm simulated size.

## CONCLUSIONS

A new type of mini multi-element TEPC based on a GEM has been designed and constructed, showing that the GEM detector may have important applications in the field of microdosimetry. Measurements performed with a <sup>137</sup>Cs source have proved that the GEM-TEPC can be operated with pure propane gas at low pressure, in order to simulate a tissue site of about 1 μm equivalent size, at a quite high gain, allowing to acquire a large part of the microdosimetric spectrum in a photon field.

Actually, measurements in a neutron field have been performed at a lower gas gain, due to limitation in the dynamic range of the digitizer. Despite this fact, the measured spectra were in

excellent agreement with those acquired by others with different kind of TEPC. Measurements performed by varying the bias voltage of the GEM, which regulate the multiplication process, have proved that this do not affect the microdosimetric information measured by the detector. Spectra measured by the GEM-TEPC do not seem therefore to be affected by those distortions in the high-y part of the microdosimetric spectra which have been measured by mini-TEPC when the applied voltage exceeds a threshold value<sup>(29)</sup>. To confirm this hypothesis, the response of the counter should be further investigated by performing measurements with higher gas gain, using an acquisition system with a wider dynamic range.

Because of the relative simple design and construction, the GEM-TEPC is therefore a good alternative to mini-TEPCs to perform microdosimetric measurements in high intensity radiation field. Besides, many microdosimetric spectra can be acquired independently, opening the experimental way to a two dimensional microdosimetric mapping of a radiation field. Furthermore, the GEM-TEPC could play an important role in the measurements of energy deposition in small simulated site sizes, which are important for an improved understanding of the biological effects of densely ionising radiation<sup>(30)</sup>. In fact, while with single wire TEPCs the energy resolution becomes unacceptably poor when operating at pressures low enough to simulate diameters lower than some hundreds of nanometres, due to the enlargement of the electronic avalanche region<sup>(31)</sup>, the separation between drift volume and charge multiplication region obtained with a TEPC based on GEM allows measurements simulating some tens of nanometres with a good energy resolution<sup>(32-33)</sup>.

## FUNDING

This work was supported and funded by the 5<sup>th</sup> Scientific Commission of the Istituto Nazionale di Fisica Nucleare (INFN) of Italy, within the framework of the MITRA research project.

## REFERENCES

1. International Commission on Radiation Units and Measurements. *Microdosimetry*. ICRU Report 36. (Bethesda: International Commission on Radiation Units and Measurements) (1983).
2. Loncol, T., Cosgrove, V., Denis, J.M., Gueulette, J., Mazal, A., Menzel, H.G., Pihet, P. and Sabattier, R. Radiobiological effectiveness of radiation beams with broad LET spectra: microdosimetric analysis using biological weighting functions. *Radiat. Prot. Dosim.* **52**, 347-352 (1994).
3. Langen, K.M., Binns, P.J., Lennox, A.J., Kroc, T.K. and DeLuca, P.M. Jr. *Pileup correction of microdosimetric spectra*. *Nucl. Instrum. Methods Phys. Res. A* **484**, 595-612 (2002).



4. Burmeister, J., Kota, C., Maughan, R.L., Waker, A.J. *Characterization of miniature tissue-equivalent proportional counters for neutron radiotherapy applications*. Phys. Med. Biol. **47**, 1633-45 (2002).
5. Kliauga, P. Measurement of single event energy deposition spectra at 5 nm to 250 nm simulated site sizes. Radiat. Prot. Dosim. **31**, 119-123 (1990).
6. Kliauga, P., Waker, A.J. and Barthe, J. *Design of tissue-equivalent proportional counters*. Radiat. Prot. Dosim. **61**, 309-322 (1995).
7. De Nardo, L., Cesari, V., Donà, G., Magrin, G., Colautti, P., Conte, V. and Tornielli, G. *Mini-TEPCs for radiation therapy*. Radiat. Prot. Dos. **108**, 345-35 (2004).
8. Kellerer, A.M. *Analysis of patterns of energy distribution*. Euratom Report, EUR 4522, d-e-f, presented at the Second Symposium on Microdosimetry, Brussels p. 107 (1970).
9. Eickel, R., Booz, J. The influence of the counter wall and the counter shape on the spectral energy deposition in small volumes by  $^{60}\text{Co}$  gamma-rays and 200 kV X-rays. Radiat. Environ. Biophys. **13**, 145-165 (1976).
10. Kellerer, A.M. Criteria for the Equivalence of Spherical and Cylindrical Proportional Counters in Microdosimetry. Radiat. Res. **86**, 277-286 (1981).
11. Rosenfeld, A.B., Bradley, P.D., Cornelius, I., Kaplan, G.I., Allen, B.J., Flanz, J.B., Goitein, M., Van Meerbeeck, A., Schubert, J., Bailey, J., Takada, Y., Maruhashi, A., Hayakawa, Y. *A new silicon detector for microdosimetry applications in proton therapy*. IEEE Trans. Nucl. Sci. **47**, 1386-94 (2000).
12. Agosteo, S., Dal Corso, F., Fazzi, A., Gonella, F., Introini, M.V., Lippi, I., Lorenzoli, M., Pegoraro, M., Pola, A., Varoli, V., Zotto, P. *The INFN Micro-Si experiment: A silicon microdosimeter for assessing radiation quality of hadrontherapy beams*. AIP Conference Proceedings **1530**, 148; doi: 10.1063/1.4812917 (2013).

13. Rollet, S., Angelone, M., Magrin, G., Marinelli, M., Milani, E., Pillon, M., Prestopino, G., Verona, C. and Verona-Rinati, G. *A novel microdosimeter based upon artificial single crystal diamond*. IEEE Trans.Nucl. Sci. **59**, 2409–15 (2012).
14. Sauli, F. *GEM: A new concept for electron amplification in gas detectors*. Nucl. Instrum. Methods Phys. Res. A **386**, 531-534 (1997).
15. Farahmand, M., Bos, A. J. J., Huizenga, J., De Nardo, L. and van Eijk, C. W. E. *Design of a new tissue-equivalent proportional counter based on a gas electron multiplier*. Nucl. Instrum. Methods Phys. Res. A **509**, 262-267 (2003).
16. Dubeau, J., Waker, A.J. *Neutron microdosimetric response of a gas electron multiplier*. Radiat. Prot. Dosim. **128**, 413-420 (2008).
17. Orchard, G.M., Chin, K., Prestwich, W.V., Waker, A.J., Byun, S.H. *Development of a thick gas electron multiplier for microdosimetry*. Nucl. Instrum. Methods Phys. Res. A **638**, 122-126 (2011).
18. Kellerer, A.M. Considerations on the random traversal of convex bodies and solutions for general cylinders. Radiat. Res. **47**, 359-376 (1971).
19. Tsuda, S., Sato, T., Takahashi, F., Satoh, D. Endo, A., Sasaki, S., Namito, Y., Iwase, H., Ban, S. and Takada, M. *Measurement of microdosimetric spectra with a wall-less tissue-equivalent proportional counter for a 290 MeV/u<sup>12</sup>C beam*. Phys. Med. Biol. **55**, 5089-5101 (2010).
20. De Nardo, L., Farahmand, M. Operation of Gas Electron Multiplier (GEM) with propane gas at low pressure and comparison with Tissue-Equivalent Gas Mixtures. Nucl. Instrum. Methods Phys. Res. A **819**, 154-162 (2016).
21. Chiriotti, S., Moro, D., Conte, V., Colautti, P., Grosswendt, B. *Equivalence of pure propane and propane TE gases for microdosimetric measurements*. Radiat. Prot. Dosim. **166**, 242-246 (2015).
22. De Nardo, L., Alkaa, A., Khamphan, C., Conte, V., Colautti, P., Ségur, P. and Tornielli G. *A detector for track-nanodosimetry*. Nucl. Instrum. Methods Phys. Res. A **484**, 312-326 (2002).

23. Bachmann, S., Bressan, A., Ropelewski, L., Sauli, F., Sharma, A., MoKrmann, D. *Charge amplification and transfer processes in the gas electron multiplier*. Nucl. Instrum. Methods Phys. Res. A **438**, 376-408 (1999).
24. Waker, A.J. *Principles of Experimental Microdosimetry*. Radiat. Prot. Dosim. **61**, 297-308 (1995)
25. Conte, V., Moro, D., Grosswendt, B. and Colautti, P. Lineal Energy Calibration Of Mini Tissue Equivalent Gas-Proportional Counters (TEPC). AIP Conf. Proc. **1530** (2013).
26. Moro, D., Chiriotti, S., Conte, V., Colautti, P. and Grosswendt, B. *Lineal energy calibration of a spherical TEPC* Radiat. Prot. Dosim. **166**, 233-237 (2015).
27. International Commission on Radiation Units and Measurements. *Stopping Powers and Ranges for Protons and Alpha Particles*. ICRU Report **49** (1993).
28. Moro, D., Chiriotti, S. *EuTEPC: measurements in gamma and neutron fields*. Radiat. Prot. Dosim. **166**, 266-70 (2015).
29. Motisi, E. Development of Microdosimetric Techniques Applied to Hadron Therapy. Master Thesis University of Padua a.a. 2014-2015.
30. Lindborg, L., Hultqvist, M, Carlsson Tedgren, Å and Nikjoo, H. *Lineal energy and radiation quality in radiation therapy: model calculations and comparison with experiment*. Phys. Med. Biol. **58**, 3089 (2013).
31. Cesari, V., Colautti, P., Magrin, G., De Nardo, L., Back, W. Y., Grosswendt, B., Alkaa, A., Khamphan, C., Ségur, P. and Tornielli G. *Nanodosimetric measurements with an avalanche confinement TEPC*. Radiat. Prot. Dosim. **99**, 337-342 (2002).
32. Farahmand M., Bos A.J.J., van Eijk C.W.E. *Gas electron multiplier (GEM) operation with tissue-equivalent gases at various pressures*. Nucl. Instrum. Methods Phys. Res. A **506**, 160-165 (2003).

33. Farahmand, M., De Nardo, L. *Microdosimetric measurements of a Tissue Equivalent Proportional Counter (TEPC) based on a Gas Electron Multiplier (GEM) down to 140 nm simulated site sizes.* Radiat. Prot. Dosim. doi: 10.1093/rpd/ncv399 (2015)

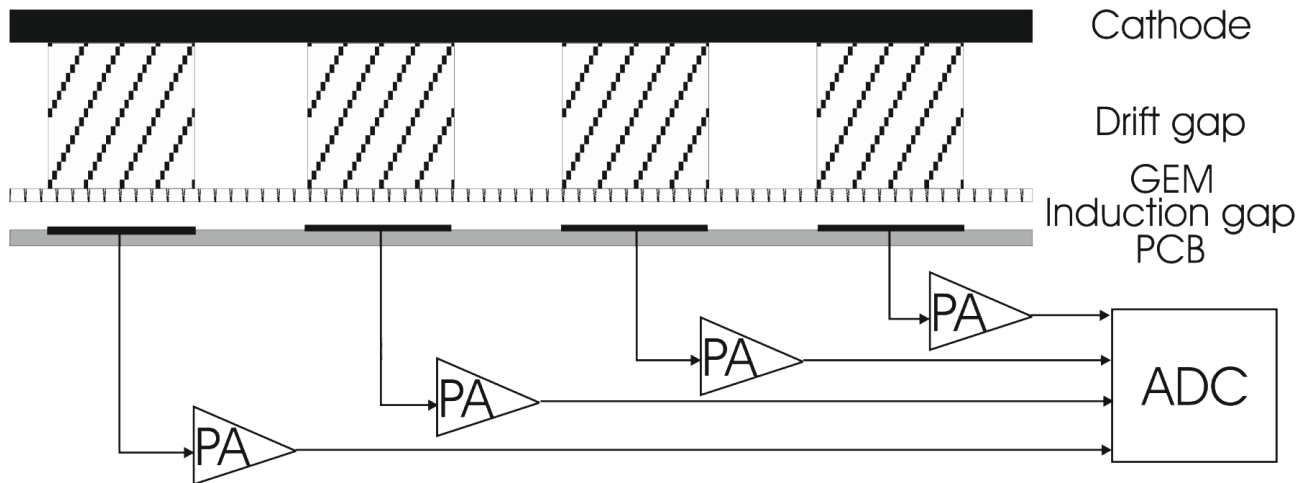


Figure 1. Cross section (not to scale) of the GEM-TEPC. The shadow areas represent four of the 16 SVs of the detector. In these measurements signals coming from four SVs were acquired.

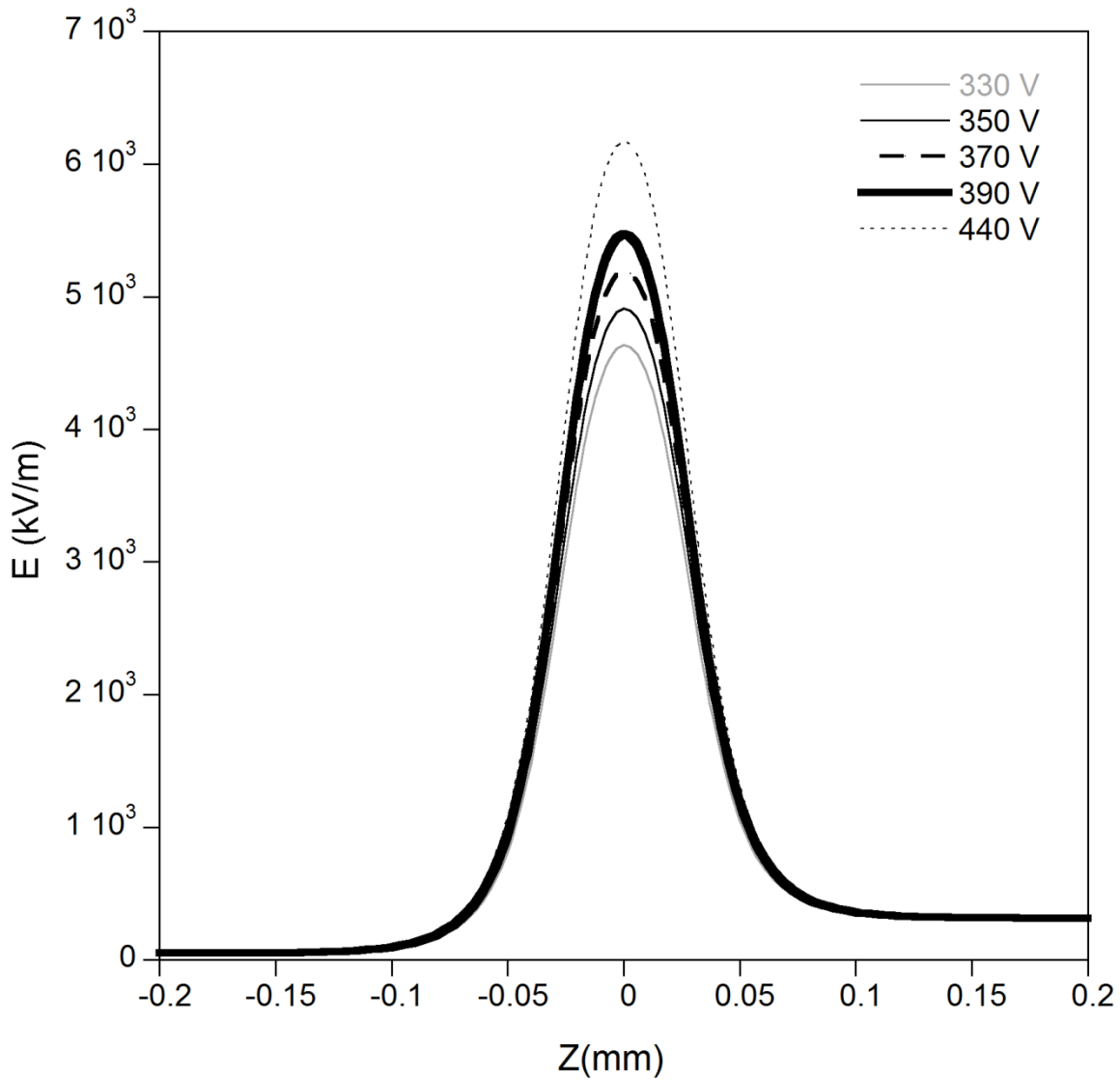


Figure 2. Electric field computed along a line perpendicular to the GEM plane and passing through the centre of the GEM hole, as a function of the distance  $Z$  from the centre of the GEM (positive and negative values of  $Z$  are toward the induction and drift regions, respectively), for different values of the voltage difference across the GEM electrodes,  $\Delta V_{GEM}$ , and fixed values of the drift and induction field ( $E_D = 45 \text{ kV}\cdot\text{m}^{-1}$  and  $E_I = 300 \text{ kV}\cdot\text{m}^{-1}$ , respectively).

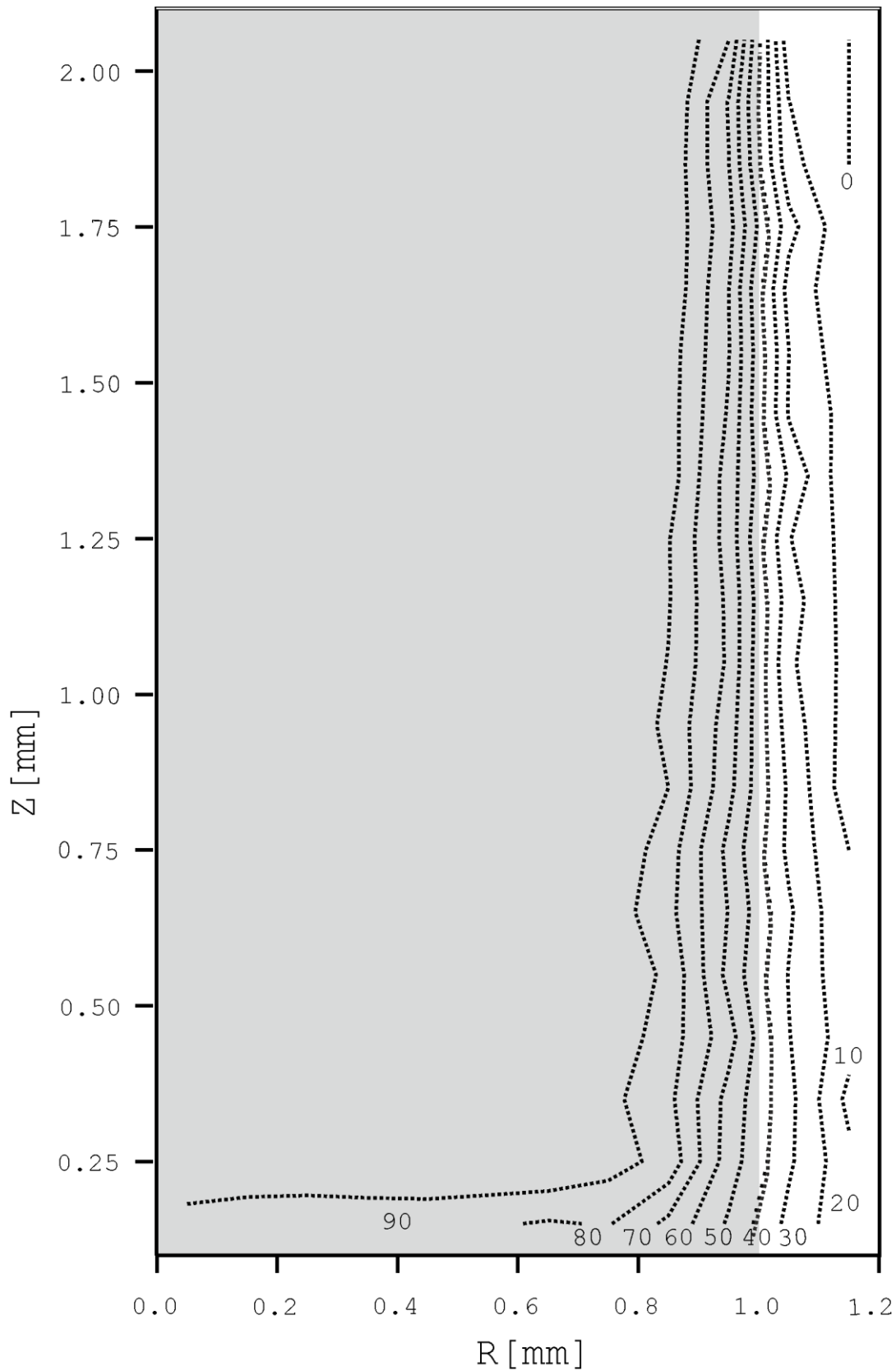


Figure 3. Calculated electron collection percentage efficiency map in C<sub>3</sub>H<sub>8</sub> at 21 kPa. The equiefficiency lines are plotted with a 10% increment. The zero coordinate for R is on the rotational axis of the cylindrical SV, the zero coordinate for Z is on the bottom of the SV, close to the cathode. The gray area point out the nominal SV, in which the average efficiency  $\bar{\epsilon}$  is calculated.

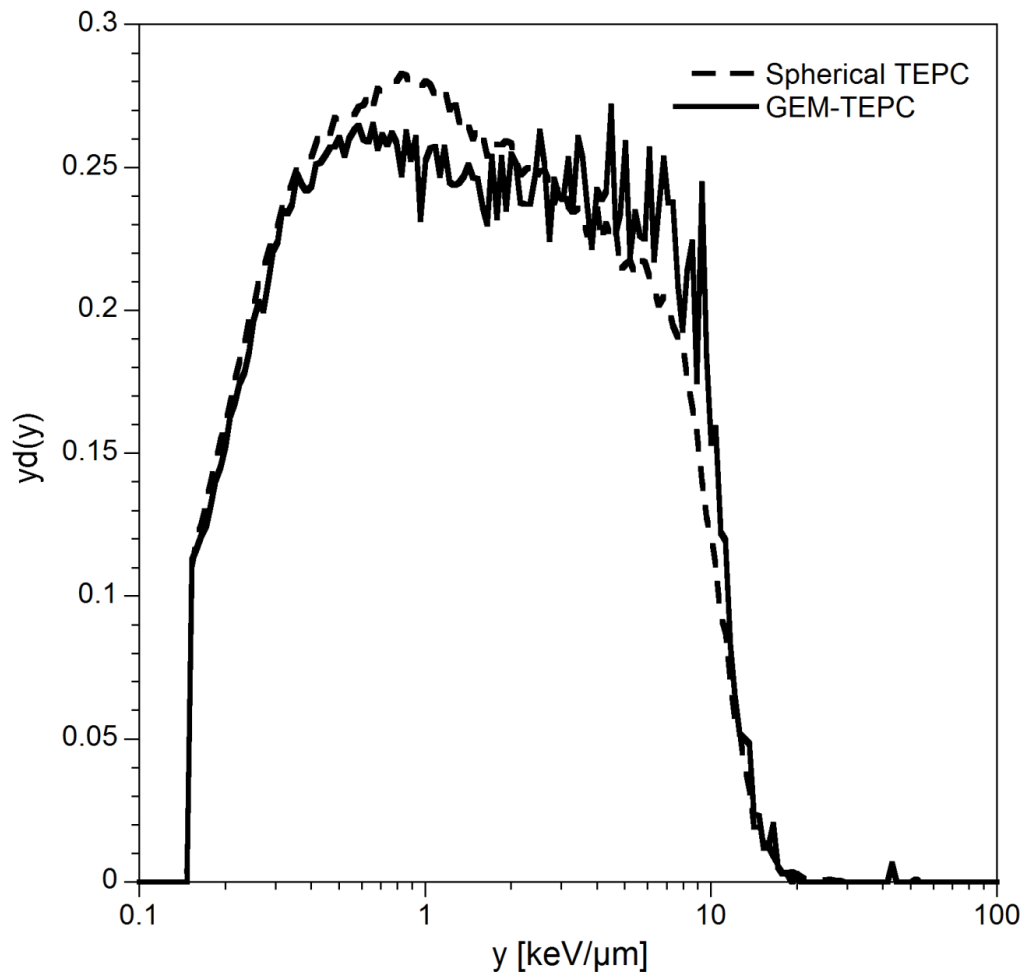


Figure 4.  $^{137}\text{Cs}$  microdosimetric spectra measured with the GEM-TEPC and with a spherical TEPC at  $1.3\ \mu\text{m}$  simulated size.

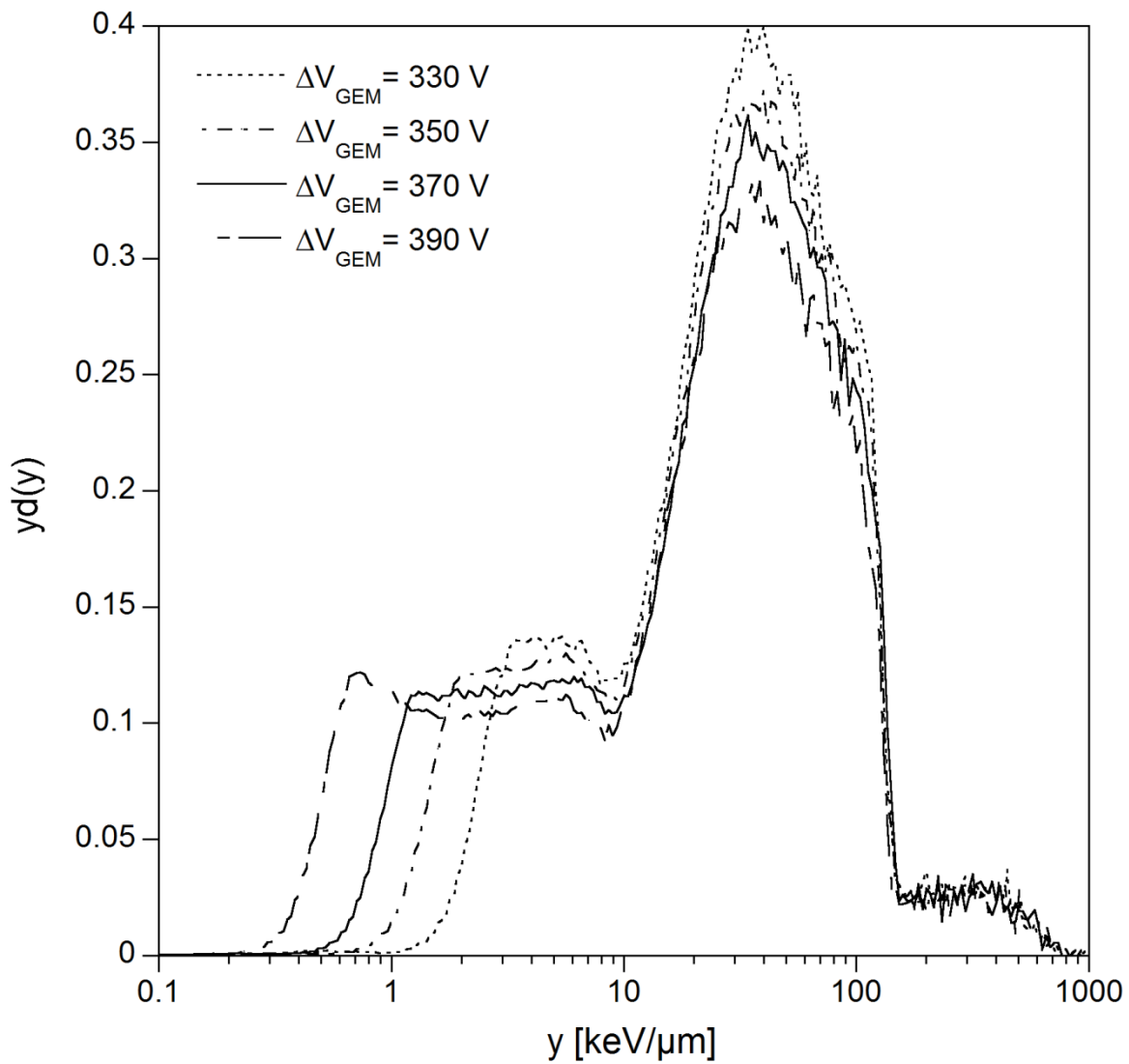


Figure 5. Microdosimetric spectra measured in a neutron field with the GEM-TEPC at 1.0  $\mu\text{m}$  simulated size for different  $\Delta V_{GEM}$ .



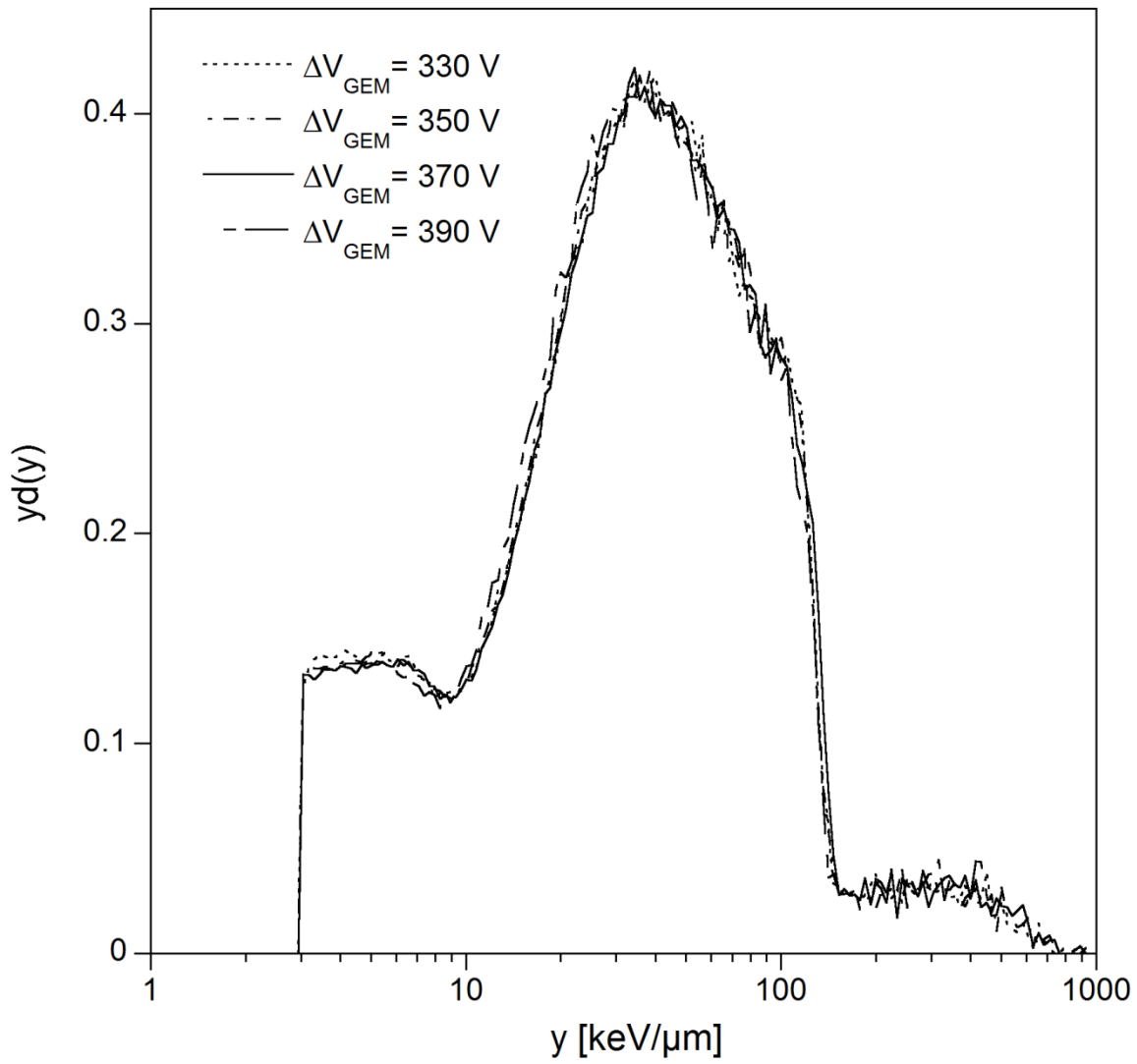


Figure 6. Microdosimetric spectra measured in a neutron field with the GEM-TEPC at 1.0  $\mu\text{m}$  simulated size for different  $\Delta V_{\text{GEM}}$ , normalised with a threshold at 3 keV/ $\mu\text{m}$ .

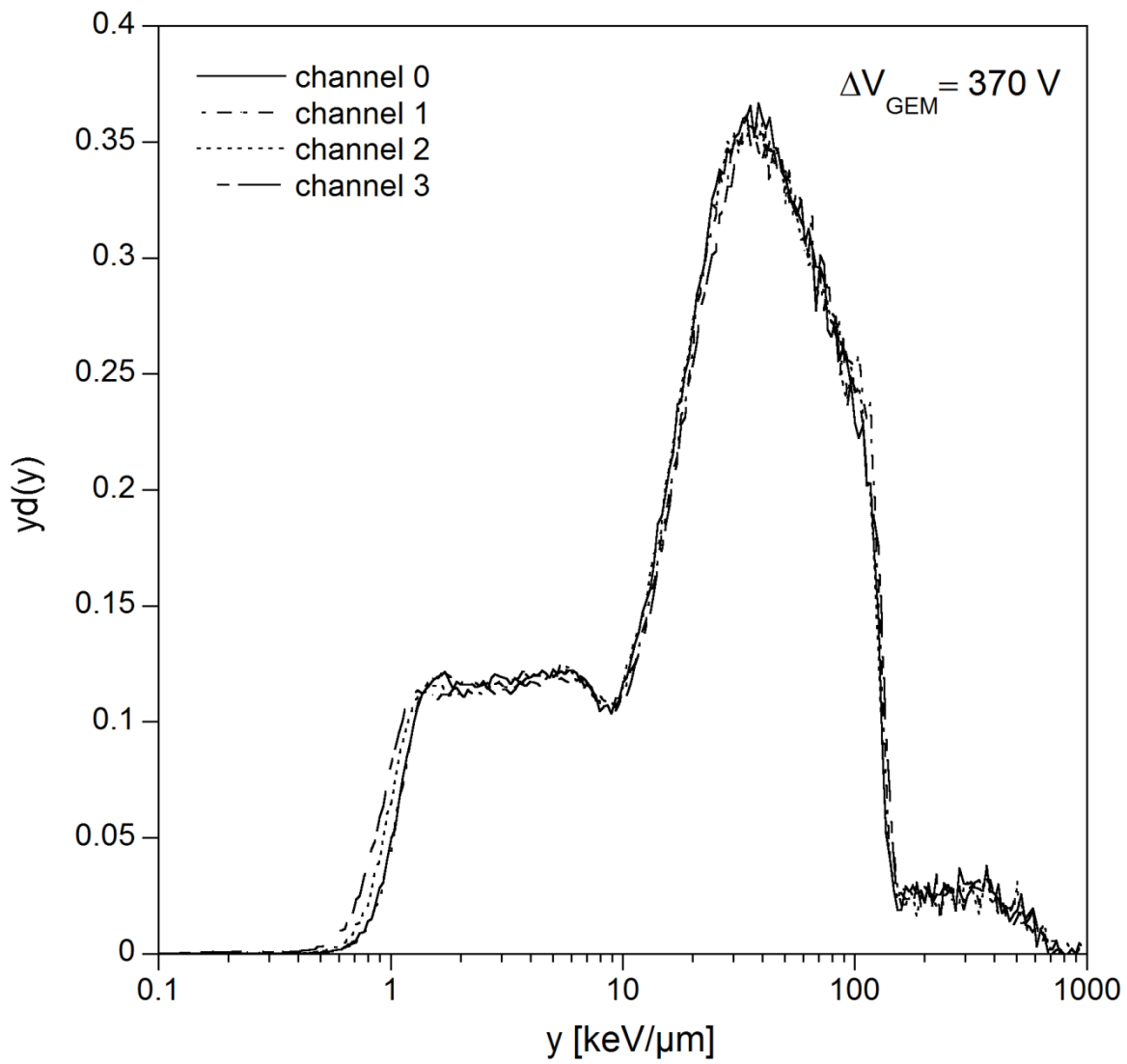


Figure 7. Microdosimetric spectra measured in a neutron field for four different SVs of the GEM-TEPC at 1.0  $\mu\text{m}$  simulated size, for  $\Delta V_{\text{GEM}}$  equal to 370V.

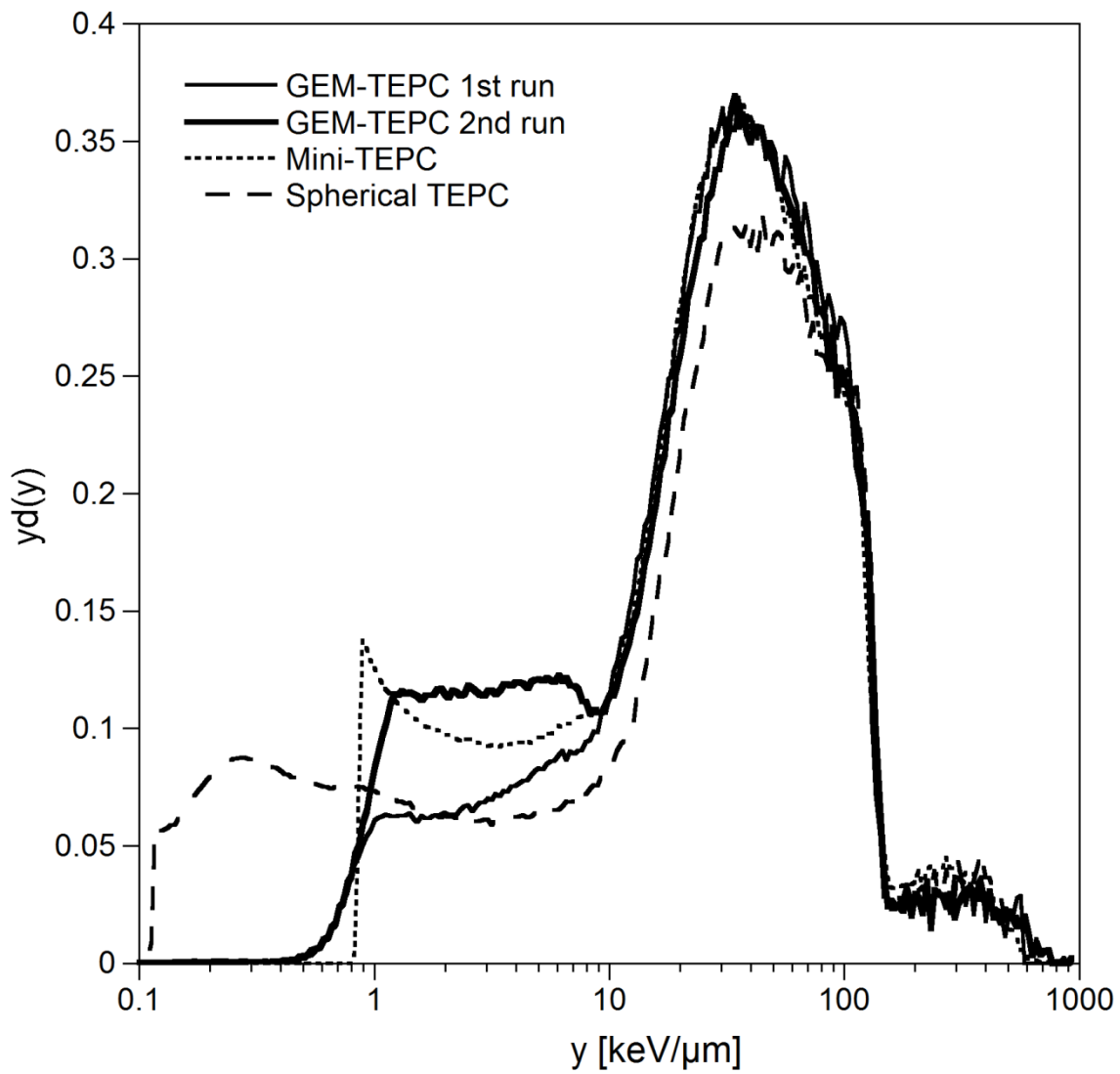


Figure 8. Microdosimetric spectra measured with the GEM-TEPC in two different runs of measurements compared with spectra acquired in the same neutron field with a mini-TEPC and with a spherical TEPC at 1.0  $\mu\text{m}$  simulated size.